Noncoherent Frequency Shift Keying for Ambient Backscatter over OFDM Signals

Mohamed ElMossallamy*, Zhu Han*◇, Miao Pan*, Riku Jäntti†, Karim Seddik‡ and Geoffrey Ye Li§

*Electrical and Computer Engineering Department, University of Houston, TX 77004, USA
◇Department of Computer Science and Engineering, Kyung Hee University, Seoul, South Korea
†Department of Communications and Networking, Aalto University, Espoo, Finland
‡Electronics and Communications Engineering Department, American University in Cairo, AUC Avenue, New Cairo 11835, Egypt
§School of Electrical and Computer Engineering, Georgia Institute of Technology, Atlanta, GA, USA

***Abstract*—In this paper, we investigate binary frequency shift keying (BFSK) over ambient OFDM signals. By cycling through a sequence of antenna loads providing different phase shifts at the tag, we are able to unidirectionally shift the ambient spectrum either up or down in frequency allowing the implementation of BFSK. We exploit the guard band and the orthogonality of the OFDM subcarriers to avoid both direct-link and adjacent channel interference. Different from energy detection based techniques which suffer from asymmetric error probabilities, the proposed scheme has symmetric error probabilities. Furthermore, we analyze the error performance of the optimal noncoherent detector and obtain an exact expression for the average probability of error. Finally, simulation results corroborate our analysis and show that the proposed scheme outperforms energy detection based schemes available in the literature by up to 3 dB.**

***Index Terms*—Ambient backscatter, internet of things, green communications, performance analysis, OFDM.**

I. Introduction

Future Internet of Things (IoT) networks are envisioned to possess billions of devices many of whom will be severely constrained in cost and power. To realize this vision, new low-cost and energy efficient communication techniques are needed. Backscatter radio is one of the main contenders to meet this fierce demand for connectivity. In traditional backscatter radio systems, ultra-low power devices commonly referred to as tags, are able to communicate by merely connecting its antenna to different loads to reflect and phase shift impinging RF signals to a reader device. Thus, all power hungry signal processing is consolidated in the reader allowing ultra-low power tags without many of the power hungry active RF components, e.g. ADCs and power amplifiers. However, traditional backscatter radio systems, e.g. RFID, require dedicated infrastructure to provide clean constant illumination for tags to communicate.

To alleviate the need for dedicated infrastructure, it has been proposed in [1] to use the existing ambient RF transmission from traditional TV, WiFi and cellular networks to illuminate backscatter tags. If we are able to piggyback information over ambient RF signals, then ubiquitous ultra-low power radio communications is within reach since RF transmissions are omnipresent. However, using already modulated RF signals for backscatter poses many challenges.

Over the last few years, many smart signaling techniques for ambient backscatter have been proposed. Early prototypes in [1]–[5] proved ambient backscatter is a viable technology. In [1], ambient TV transmissions have been exploited to establish a link between two battery-less tags. By backscattering at a much lower rate than the high bandwidth TV signal, a simple averaging detector has been used to decode the tag's information. Improved bit rates and communication range have been achieved in [2] by mitigating the direct interference coming directly from the ambient source and using more robust orthogonal spread spectrum signaling. In [3], bi-directional Internet connectivity has been achieved between a tag and a commercial off-the-shelf WiFi device. This has been enabled by received signal strength indicator (RSSI) measurements in the uplink and energy detection of short WiFi packets in the downlink. In [4], coherent phase shift keying has been used, enabled by a modified full-duplex-capable WiFi AP that is able to cancel direct link interference and estimate the channel. In [5], Bluetooth and WiFi signals have been shifted to the two adjacent channels using rapid On-off Keying (OOK) and have been received using commodity radios. Furthermore, it has been shown in [6]–[8] that packets for multiple standards can be generated via backscatter. In [6], it has been shown that WiFi packets can be generated by backscattering modified Bluetooth packets. While in [7] and [8], respectively, FM signals and LoRa signal have been generated by backscattering ambient signals of the same modulation.

Motivated by the promising early prototypes, a slew of research investigated more theoretical aspects of ambient backscatter, such as modelling, error performance and capacity analysis [9]–[14]. It has been shown in [9] that adding backscattering nodes to a legacy MIMO communication system increases the achievable sum rate. The performance of the differential encoding and averaging detection scheme originally proposed in [1] has been investigated in the case of a single antenna at the reader in [10] and multiple antennas in [11]. More research focusing either on noncoherent or semi-coherent detection performance of ambient backscatter can be found in [12], [13]. Most of the previous works assume no

This work is partially supported by US MURI AFOSR MURI 18RT0073, NSF CNS-1717454, CNS- 1731424, CNS-1702850, CNS-1646607.

978-1-5386-8088-9/19/$31.00 ©2019 IEEE

specific modulation for the ambient source and rely heavily on Gaussian approximations.

Since most current wireless systems rely on orthogonal frequency division multiplexing (OFDM), there have been some efforts to exploit the structure of the OFDM waveform to provide more robust ambient backscatter communications. In [14], the remaining part of cyclic prefix has been used to cancel direct-link interference. While in [15], the orthogonality of the OFDM subcarriers has been exploited to avoid direct link interference by shifting backscattered energy to null subcarriers. The two aforementioned schemes rely on energy detection and suffer from asymmetric error performance and cumbersome threshold estimation. Finally, it has been shown in [16] that ambient backscatter can also benefit legacy OFDM transmissions by offering a form of diversity.

In this paper, we investigate binary frequency shift keying over ambient OFDM signals. Our contributions in this paper can be summarized as follows:

- We propose a backscatter technique that allows binary frequency shift keying modulation over ambient OFDM carriers. Different from other frequency shifting techniques that rely on on-off keying to shift backscattered energy to adjacent channels on both sides of the ambient signal, we propose a frequency shifting technique that relies on cycling through the phase shifts of a complex sinusoid allowing unidirectional frequency shift without causing sidebands or undesired frequency components.
- We analyze the optimal noncoherent detector and obtain an exact expression for the average probability of error. Different from schemes that rely on energy detection [14], [15], our optimal detector has symmetric error probabilities for '0's and '1's and does not require the estimation of an SNR-dependent threshold.
- We provide simulation results to verify our analysis and study the effects of system parameters, namely, the maximum channel delay spread, and OFDM symbol size, on the error performance. Our results show the proposed scheme outperforms energy detection based schemes in [14], [15].

The rest of the paper is organized as follows. In Section II, we outline our system model. In Section III, we introduce our ambient backscatter modulation scheme, study the optimal detector and analyze the error performance. In Section IV, we provide simulation results to verify our analysis and benchmark our proposed schemes against existing schemes in the literature. Finally, we conclude the paper in Section V.

II. System Model

We consider the classical three node ambient backscatter system model [14], [15], [17] shown in Fig. 1. In general, ambient backscatter communications rely on the existence of RF transmissions generated by an existing traditional communication system, hereinafter referred to as the *legacy* communications system. We assume the legacy communication system employs OFDM. e.g. LTE or WiFi. The legacy communication nodes possess traditional active transceivers

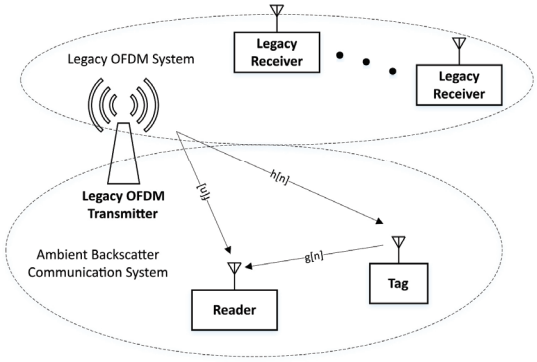

Fig. 1. System Model

powered by large capacity batteries or connected to the power grid and thus are unaffected by the weaker backscattered signals. On the other hand, the ambient backscatter communication system consists of ultra-low power tags that communicate by changing their antenna loads to backscatter ambient signals back to a reader device. The tags can rely only on energy harvesting to support their operation, while the reader is a traditional radio transceiver.

Assume there are one ambient source, one tag, and one reader, each with a single antenna, and all channels are mutually independent multipath Rayleigh fading channels. Let $f(t)$, $h(t)$ and $g(t)$ denote the channel impulse responses between the ambient source and the reader, the ambient source and the tags, and the tag and the reader, respectively. The corresponding delay spreads are given by τ_f, τ_h and τ_g.

The bandpass signal emitted from the legacy transmitter can be written as

$$s(t) = \Re\left\{\sqrt{\rho}\; s_l(t)\, \mathrm{e}^{j2\pi f_c t}\right\}, \tag{1}$$

where $\Re\{\cdot\}$ denotes the real-part operator, ρ is the average transmitted power, $s_l(t)$ is the baseband representation of $s(t)$, and f_c is the center frequency. Hence, the signal received at the tag is given by

$$x(t) = \Re\left\{\left[\sqrt{\rho}\; s_l(t) * h_l(t)\right] \mathrm{e}^{j2\pi f_c t}\right\}, \tag{2}$$

where $*$ denote linear convolution, and $x_l(t) = \sqrt{\rho} s_l(t) * h_l(t)$ is the baseband representation of $x(t)$.

The tag modulates its information by simply connecting its antenna to different loads. Hence, no thermal noise is added at the tag [10], [11], [14]. Let $b_l(t)$ denote the baseband representation of the tag's modulation waveform with corresponding bandpass signal $b(t)$ and α denote the tag reflection coefficient. The received signal at the reader can be written as

$$y(t) = \underbrace{\left[\alpha x(t)\, b(t)\right] * g(t)}_{y^b(t)} + \underbrace{s(t) * f(t)}_{y^d(t)} + w(t), \tag{3}$$

where $y^b(t) = [\alpha x(t)\, b(t)] * g(t)$ is the signal backscattered from the tag, $y^d(t) = s(t) * f(t)$ is the signal received directly from the legacy transmitter, and $w(t)$ is bandpass Gaussian noise, which is independent of both $y^b(t)$ and $y^d(t)$. Note that tag's information in present only in the term

$y^b(t)$, while $y^d(t)$ is the direct-link (i.e. legacy-transmitter to reader) interference. The baseband representation of the received signal can be written as

$$y_l(t) = y_l^b(t) + y_l^d(t) + w_l(t), \tag{4}$$

where $y_l^b(t)$, $y_l^d(t)$, and $w_l(t)$ denote the baseband representations of $y^b(t)$, $y^d(t)$, and $w(t)$, respectively.

At the reader, the received signal is down-converted to baseband and passed through an analog-to-digital converter (ADC). Let N_f denote the number of subcarriers, or equivalently the length of the fast Fourier transform (FFT), and N_{cp} denote the cyclic prefix length. The resultant discrete-time baseband sequence for one OFDM symbol can be written as

$$y_l[n] = y_l^b[n] + y_l^d[n] + w_l[n], \quad n = 1, 2, \ldots, N_f + N_{cp}, \tag{5}$$

where $w_l[n]$ is complex baseband additive white Gaussian noise (AWGN) with zero-mean and variance σ_w^2. Let $h_l[n]$, $f_l[n]$, and $g_l[n]$ denote the discrete-time baseband representation of $h(t)$, $f(t)$, and $g(t)$, respectively, whose lengths are given by $L_h = \lfloor \tau_h f_s \rfloor$, $L_f = \lfloor \tau_f f_s \rfloor$, and $L_g = \lfloor \tau_g f_s \rfloor$, where f_s is the sampling frequency. Let $\tau \triangleq \max\{\tau_f, \tau_h + \tau_g\}$ denote the maximum channel delay spread; hence, $L \triangleq \max\{L_f, L_h + L_g - 1\}$ denotes the discrete-time length of maximum channel delay spread. Moreover, in practice the tag-reader distance is fairly small and it is reasonable to assume $L_g = 1$ [14]. Then, we can write $y_l^b[n] = g x_l[n] b_l[n]$ and $y_l^d[n] = \sqrt{p} s_l[n] * f_l[n]$. In the rest of the paper, we use the discrete-time baseband model and drop the subscript l for notational convenience.

Our goal is to design the tag modulation to allow completely noncoherent detection of $b[n]$ from the received signal $y[n]$ without knowing either the transmitted OFDM symbol $s[n]$, the relevant channels $h[n], f[n]$, and g or even the average SNR.

III. Transceiver Design and Performance Analysis

In this section, we propose a frequency shift keying modulation scheme for backscatter communications over ambient OFDM signals. We describe the tag modulation waveform and study the optimal noncoherent detector. We also analyze the error performance of the proposed scheme and obtain an analytical expression for the average error probability.

A. Tag Waveform Design

In OFDM systems, a number of subcarriers along the edges of the spectrum, but still inside the channel bandwidth, are left null to serve as a guard band and satisfy FCC spectrum masks. Recently, these guard bands have been proposed as one of the deployment options for narrow band IoT (NB-IoT) [18]. The number of those subcarriers will depend on the channel bandwidth and the subcarriers spacing. For example, a 10 MHz LTE waveform has 64 inband null subcarriers along the edges [19]. Let $\mathcal{U}$ and $\mathcal{L}$ denote the set of upper guard subcarriers and the set of lower guard subcarriers, respectively. "upper" refers to subcarriers above the center frequency and "lower" refers to subcarriers below the center frequency. In practice, the number of upper and lower subcarriers will be equal. Hence, we assume $|\mathcal{U}| = |\mathcal{L}| = N$, where $|\cdot|$ denote the cardinality of a set.

We design the tag modulation waveform to take advantage of these guard band subcarriers and the orthogonality inherent in the OFDM waveform to overcome direct-link interference, while allowing very simple square-law detection without an SNR dependent threshold. In particular, the tag modulation waveform selectively shifts the spectrum of the backscattered signal to either the upper or lower guard bands to transmit one bit of information. Hence, the detector can simply compare the energy in the two bands to decode the tag information. The detector does not need to know the transmitted OFDM symbol, any of the relevant channels or even set an SNR-dependent threshold. This scheme can be viewed as over-imposing binary frequency-shift keying (BFSK) on top of the ambient signal. We propose a simple implementation that ensures no backscatter energy is shifted outside the channel bandwidth.

Let every backscatter symbol span the duration of one legacy OFDM symbol [14], [16]. The tag uses the following waveform to convey one information bit per OFDM symbol,

$$b[n] \triangleq \begin{cases} \mathrm{e}^{i2\pi \frac{N}{N_f} n}, & B = 0, \\ \mathrm{e}^{-i2\pi \frac{N}{N_f} n}, & B = 1, \end{cases} \tag{6}$$

where $n = 1, 2, \ldots, N_f + N_{cp}$ and $B \in \{0, 1\}$ is the information bit being transmitted. Hence, to transmit a '1' bit the tag will connect its antenna to different loads to cycle through a specific number of fixed phase shifts in one direction (order), while to transmit a '0' bit the tag will cycle through the same antenna loads but in the opposite direction (order). Implementing these phase shifts is a well-studied problem, originally encountered in the implementation of phase shift keying in backscatter tags. One implementation in the context of ambient backscatter can be found in [4]. By simply cycling through the phase shifts we can implement complex sinusoids and unidirectionally shift the spectrum of the ambient signal up or down in frequency. Note that unlike [5], [20], the proposed technique enables unidirectional frequency shifts without sidebands or unwanted frequency components from mixing and all backscattered energy is retained inside the channel bandwidth avoiding adjacent channel interference.

The backscattered signal received at the reader can be written as

$$y^b[n] = \begin{cases} \alpha g\, x[n]\, \mathrm{e}^{i2\pi \frac{N}{N_f} n}, & B = 0, \\ \alpha g\, x[n]\, \mathrm{e}^{-i2\pi \frac{N}{N_f} n}, & B = 1. \end{cases} \tag{7}$$

Taking the discrete Fourier transform of (7), the backscattered signal spectrum can be written as

$$Y^b[m] = \begin{cases} \alpha g X[m] \circledast \delta[m - N] = \alpha g\, X[m - N], & B = 0, \\ \alpha g X[m] \circledast \delta[m + N] = \alpha g\, X[m + N], & B = 1, \end{cases} \tag{8}$$

where $\circledast$ denotes circular convolution, and $X[m]$ is the discrete Fourier transform (DFT) of $x[n]$. Thus, from the

viewpoint of the frequency domain, to transmit a '0' bit, the tag shifts the spectrum of the backscattered signal into the upper guardband, $\mathcal{U}$, while to send a '1', the tag shifts the spectrum of the backscattered signal into the lower guardband, $\mathcal{L}$.

B. Detector

In practice, the ambient backscatter receiver will not have knowledge of the ambient OFDM signal, $s[n]$ or any of the relevant channels, $h[n]$, $f[n]$, or g. Hence, we will have to resort to noncoherent detection. In the case of noncoherent FSK, the square-law detector is actually known to be optimal [21]. Different from energy detection based schemes in [14], [15], this detector does not rely on a threshold and does not need to estimate the average SNR. The proposed detector requires the receiver to only have knowledge of the set of upper and lower guard subcarriers. Moreover, we will show that it has symmetric error probabilities for '0's and '1's, which is another major advantage over energy detection based schemes.

Let $Y[m]$ denote the output of the FFT at the receiver. Then we can write two test statistics, one for the upper guardband, $\mathcal{U}$, as

$$E_u = \frac{2}{\sigma_w^2} \sum_{m \in \mathcal{U}} |Y[m]|^2, \tag{9}$$

and one for the lower guardband, $\mathcal{L}$, as

$$E_l = \frac{2}{\sigma_w^2} \sum_{m \in \mathcal{L}} |Y[m]|^2. \tag{10}$$

Based on these test statistics, we can simply write our detection rule as

$$\hat{B} = \begin{cases} 0, & E_u > E_l, \\ 1, & E_l \geq E_u. \end{cases} \tag{11}$$

Since the direct link signal exists only on the data subcarriers, neither E_u nor E_l suffers from direct link interference. Note that, contingent on the transmitted bit, E_u and E_l may depend on the random backscatter channels, $h[n]$ and g. Next, we analyze the distribution of the test statistics and the received SNR.

Let $\mathcal{H}_0$ and $\mathcal{H}_1$ denote the hypotheses that the transmitted bit is '0' or '1', respectively. We first focus on $\mathcal{H}_0$, the hypothesis that the transmitted bit is a '0'. Under $\mathcal{H}_0$, the backscattered signal spectrum is shifted into the upper guard band subcarriers, $\mathcal{U}$, and the lower guard band subcarriers, $\mathcal{L}$, contain only noise. Hence, E_l is just the sum of the squares of N standard Gaussian random variables. Hence, $E_l|\mathcal{H}_0 \sim \chi^2_{2N}$, where χ^2_{2N} denote the central chi-squared variate with $2N$ degrees of freedom. On the other hand, E_u depends on the random backscatter channel. The instantaneous received signal to noise ratio in the upper guard band can be written as

$$\gamma_u = \frac{\rho |\alpha|^2 |g|^2 \sum_{m \in \mathcal{U}} |H[m]|^2}{N \sigma_w^2}, \tag{12}$$

where $\{H[m]\}_{m \in \mathcal{U}}$ are the flat-fading channel coefficients seen by the upper guard band subcarriers. Hence, conditional on the instantaneous received SNR, $E_u|\mathcal{H}_0 \sim \chi^2_{2N}(2N\gamma_u)$ where $\chi^2_{2N}(2N\gamma_u)$ is the noncentral chi-squared distribution with $2N$ degrees of freedom and noncentrality parameter $2N\gamma_u$.

Under $\mathcal{H}_1$, the backscattered signal spectrum is shifted to the lower guard band subcarriers, $\mathcal{L}$, and we have a reciprocal situation to that under $\mathcal{H}_0$. In particular, E_u is just the sum of the squares of N standard Gaussian random variables and follows the central chi-squared distribution, i.e. $E_u|\mathcal{H}_1 \sim \chi^2_{2N}$. While E_l depends on the instantaneous received SNR in the lower guard band sub-carriers which can be written as

$$\gamma_l = \frac{\rho |\alpha|^2 |g|^2 \sum_{m \in \mathcal{L}} |H[m]|^2}{N \sigma_w^2}, \tag{13}$$

where $\{H[m]\}_{m \in \mathcal{L}}$ are the flat-fading channel coefficients seen by the lower guard band subcarriers. Hence, conditional on the instantaneous received SNR, $E_l|\mathcal{H}_1 \sim \chi^2_{2N}(2N\gamma_l)$.

Note that since $\{H[m]\}_{m \in \mathcal{U}}$ and $\{H[m]\}_{m \in \mathcal{L}}$ are identically distributed, the instantaneous received SNRs in the upper and lower guard subcarriers, γ_u and γ_l, are also identically distributed. From now on, we denote the instantaneous received SNR in either bands by γ.

The instantaneous SNR, γ, is a scaled product of two random variables: $|g|^2$, which is an exponential random variable, and $q \triangleq \sum_{m \in \mathcal{U}} |H[m]|^2$ (or equivalently $\sum_{m \in \mathcal{L}} |H[m]|^2$), which is the sum of N *correlated* exponential random variables. The correlation arises from the fact that the subcarrier spacing has to be smaller than the coherence bandwidth. Let $\mathbf{h}$ denote the vector comprising the channel coefficients $\{H[m]\}_{m \in \mathcal{U}}$ (or $\{H[m]\}_{m \in \mathcal{L}}$). Then, using the technique in [22], the distribution of q can be found to be

$$p(q) = \sum_{r=1}^{R} \left(\prod_{k \neq r} \frac{\frac{1}{\lambda_k}}{\frac{1}{\lambda_k} - \frac{1}{\lambda_r}} \right) \frac{1}{\lambda_r} \mathrm{e}^{-\frac{q}{\lambda_r}}, \tag{14}$$

where $\{\lambda_r\}_{r=1}^{R}$ are the non-zero eigenvalues of the covariance matrix $E\left[\mathbf{h}\mathbf{h}^{\dagger}\right]$. Using the product distribution formula, the instantaneous SNR distribution can be readily found to be

$$p(\gamma) = \sum_{r=1}^{R} \left(\prod_{k \neq r} \frac{\frac{1}{\lambda_k}}{\frac{1}{\lambda_k} - \frac{1}{\lambda_r}} \right) \frac{2N}{\lambda_r \overline{\gamma}} \mathbf{K}_0 \left(2\sqrt{\frac{N\,\gamma}{\lambda_r\,\overline{\gamma}}} \right), \tag{15}$$

where $\overline{\gamma} \triangleq E[\gamma] = |\alpha|^2 \frac{\rho}{\sigma_w^2}$ is the average detection SNR and $\mathbf{K}_m(\cdot)$ is the modified Bessel function of the second kind and m-th order.

C. Error Performance

Next, we analyze the probability of error for the proposed scheme. Assuming the tag transmitted bits are equally probable to be ones or zeros, the probability of error is given by

$$P_e = \frac{1}{2} \left[P\left(\hat{B} = 1 | \mathcal{H}_0\right) + P\left(\hat{B} = 0 | \mathcal{H}_1\right) \right]. \tag{16}$$

which is equivalent to

$$P_e = \frac{1}{2}\left[P\left(E_l > E_u|\mathcal{H}_0\right) + P\left(E_u > E_l|\mathcal{H}_1\right)\right]. \\ = \frac{1}{2}\left[P\left(\frac{E_l}{E_u} < 1|\mathcal{H}_0\right) + P\left(\frac{E_u}{E_l} < 1|\mathcal{H}_1\right)\right]. \tag{17}$$

Note that $E_l|\mathcal{H}_0 \overset{d}{=} E_u|\mathcal{H}_1$ and $E_l|\mathcal{H}_1 \overset{d}{=} E_u|\mathcal{H}_0$, where $\overset{d}{=}$ denotes equality in distribution. Hence, unlike energy detection based techniques [14], [15], which have different false-alarm and missed-detection probabilities at the optimal threshold leading to asymmetric error performance, we have symmetric error probabilities under $\mathcal{H}_0$ and $\mathcal{H}_1$.

Since we have symmetric error probabilities, it is sufficient to find the error probability under $\mathcal{H}_0$. We already discussed the distribution of E_l and E_u in the previous subsection. Under $\mathcal{H}_0$, and conditional on the channel, E_l follows a noncentral chi-squared distribution with noncentrality parameter $2N\gamma$ and E_u follows a central chi-squared distribution, both with $2N$ degrees of freedom. Since E_l and E_u are independent, the quotient $z \triangleq \frac{E_l}{E_u}$ follows the Fisher-Snedecor *singly* noncentral F-distribution whose probability density function is given by

$$p\left(z\right) = \sum_{j=0}^{\infty} \frac{e^{\delta/2}\left(\delta/2\right)}{B\left(\frac{v_2}{2}, \frac{v_1}{2}+j\right) j!} \left(\frac{v_1}{v_2}\right)^{\frac{v_1}{2}+j} \\ \left(\frac{v_2}{v_2+v_1 z}\right)^{\frac{v_1+v_2}{2}+j} z^{\frac{v_1}{2}-1+j}, \tag{18}$$

where $B(\cdot,\cdot)$ is the beta function and v_1 and v_2 are the degrees of freedom of the numerator and denominator, respectively, and δ is the noncentrality parameter of the numerator. The cumulative distribution function is given by

$$F\left(z; v_1, v_2, \delta\right) = \sum_{j=0}^{\infty} \left(\frac{\left(\frac{\delta}{2}\right)^j}{j!} \mathrm{e}^{-\frac{\delta}{2}}\right) I\left(\frac{v_1 z}{v_2+v_1 z}|\frac{v_1}{2}+j, \frac{v_2}{2}\right), \tag{19}$$

where $I\left(x|a,b\right)$ is the *incomplete* beta function with parameters a and b. Hence, the instantaneous probability of error can be written as

$$P_e = F\left(1; 2N, 2N, 2N\gamma\right) \\ = \sum_{j=0}^{\infty} \left(\frac{\left(N\gamma\right)^j}{j!} \mathrm{e}^{-N\gamma}\right) I\left(\frac{1}{2}|N+j, N\right). \tag{20}$$

To get the average probability of error, we need to average the error probability in (20) over the distribution of the SNR obtained in (15). Expressing the exponential and Bessel functions in terms of the Meijer G-function, we can write the average probability of error as

$$\overline{P_e} = \sum_{j=0}^{\infty}\sum_{r=0}^{R} \frac{N^j}{j!} I\left(\frac{1}{2}|N+j, N\right) \left(\prod_{k\neq r} \frac{\frac{1}{\lambda_k}}{\frac{1}{\lambda_k}-\frac{1}{\lambda_r}}\right) \\ \times \int_0^{\infty} \gamma^{j-1} G_{0,1}^{1,0}\left(\begin{matrix}-\\0\end{matrix}\middle|\, N\gamma\right) G_{0,2}^{2,0}\left(\begin{matrix}-\\1,1\end{matrix}\middle|\, \frac{N\,\gamma}{\lambda_r\,\overline{\gamma}}\right) d\gamma. \tag{21}$$

The integral in (21) can be solved with the help of [23, 07.34.21.0011.01] to obtain the final expression for the average error probability of error as

$$\overline{P_e} = \sum_{j=0}^{\infty}\sum_{r=0}^{R} \left(\prod_{k\neq r} \frac{\frac{1}{\lambda_k}}{\frac{1}{\lambda_k}-\frac{1}{\lambda_r}}\right) \frac{I\left(\frac{1}{2}|N+j, N\right)}{j!} \\ \times G_{1,2}^{2,1}\left(\begin{matrix}1-j\\1,1\end{matrix}\middle|\, \frac{1}{\lambda_r\,\overline{\gamma}}\right). \tag{22}$$

Both the incomplete beta function and the Meijer G-function are available as built-in functions in MATLAB making the evaluation of this expression straight-forward.

IV. Results and Discussion

In this section, we evaluate the performance of the proposed scheme by computer simulations and verify the analysis carried out in Section III. In our simulation, we use the OFDM system parameters from the LTE standard. We study the effects of the OFDM symbol size and maximum channel delay spread, τ, on the error performance. Moreover, we compare our proposed scheme against the baseline energy detection based scheme from [15], which has been shown to outperform the other energy detection based scheme in [14].

The scheme in [15] also makes use of the guard band subcarriers along the edges of the OFDM symbol spectrum. In particular, to send a '1', the tag switches its antenna impedance between two states causing the spectrum of the backscattered signal to fall on both sides of the guard band. Whereas to send '0' the tag just keeps its antenna impedance constant. Hence, energy detection over the entire guard band can be used to decode the tag information. Drawbacks of that scheme are; first, the energy detector threshold will be function of the SNR, which needs to be estimated at the receiver; second, the ML detector has asymmetrical error probabilities for '0's and '1's.

In Fig. 2, we vary the OFDM symbol size, N_f, and compare the average bit-error rate of the proposed scheme against the baseline from [15] with perfect SNR estimation. We observe that the proposed scheme outperforms the baseline for all OFDM symbol sizes. This is expected as noncoherent FSK is predicted to perform better than simple energy detection. Notably, the advantage in performance also seems to increase with SNR. For example, note that for $N_f = 2048$, the proposed scheme outperforms the baseline by around 2 dB at a bit-error rate of 10^{-2}, and that advantage grows to more than 3 dB at a bit-error rate of 10^{-3}. We also observe that the error probability obtained from analytical expressions, denoted by markers, matches the simulation results which verifies our analysis in Section III.

Finally, in Fig. 3, we vary the maximum channel delay spread, τ, and compare the probability of error for the proposed scheme against the baseline. From the figure, the proposed scheme outperforms the baseline for all values of delay spread. Moreover, the proposed scheme does not seem to be greatly affected by the change in the delay spread, unlike [14] which relies on the remaining part of the cyclic prefix and fails for high values of delay spread. Again, note that the

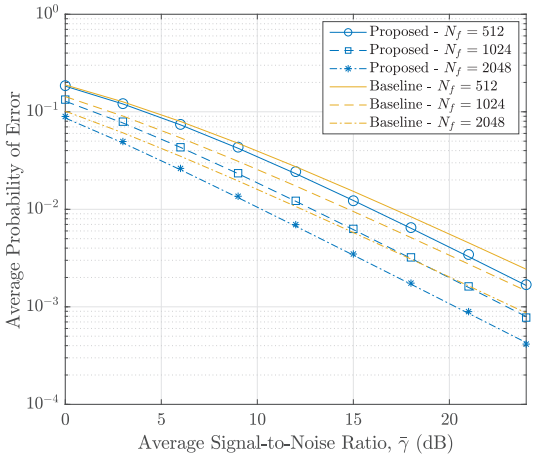

Fig. 2. Average probability of error for different OFDM carrier bandwidths, and a maximum channel delay spread, τ, of $3\mu s$. Lines correspond to Monte-Carlo simulations and markers correspond to analytical expressions. Baseline scheme from [15] is simulated.

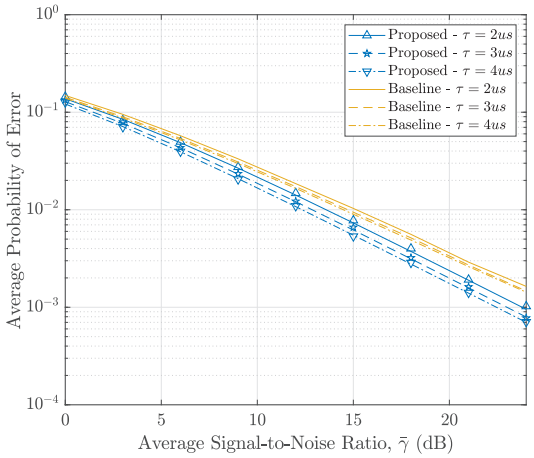

Fig. 3. Average probability of error for different values of τ. Lines correspond to Monte-Carlo simulations and markers correspond to analytical expressions. Baseline scheme from [15] is simulated. $N_f = 1024$.

analytical probability of error matches the one obtained by simulations, which verifies our analysis.

V. Conclusion

We have proposed a novel technique to implement binary frequency shift keying in backscatter systems over ambient OFDM signals. The proposed technique relies on cycling through different phase shifts to allow unidirectional band-pass frequency shifts enabling the implementation of BFSK over ambient OFDM signals. By exploiting the guardband subcarriers and the orthogonality of the OFDM waveform, we have avoided direct-link and adjacent channels' interference. Moreover, we have studied the optimal noncoherent detector and obtained an exact expression for the average probability of error. The proposed scheme avoids two drawbacks of energy detection based techniques. First, it allows simple threshold-less detection and exempts the reader from estimating the SNR. Second, it has symmetric error probabilities for '1's and '0's. Our simulation results have corroborated our analysis and showed that the proposed scheme outperforms energy detection schemes available in the literature by up to 3 dB.

References

[1] V. Liu *et al.*, "Ambient backscatter: wireless communication out of thin air," in *Proc. of the ACM SIGCOMM Conf.*, Hong Kong, China, Aug. 2013, pp. 39–50.

[2] A. N. Parks *et al.*, "Turbocharging ambient backscatter communication," in *Proc. of the ACM SIGCOMM Conf.*, Chicago, IL, Aug. 2014, pp. 619–630.

[3] B. Kellogg *et al.*, "Wi-fi backscatter: internet connectivity for RF-powered devices," in *Proc. of the ACM SIGCOMM Conf.*, Chicago, IL, Aug. 2014, pp. 607–618.

[4] D. Bharadia *et al.*, "BackFi: high throughput WiFi backscatter," in *Proc. of the ACM SIGCOMM Conf.*, London, U.K., Aug. 2015, pp. 283–296.

[5] P. Zhang *et al.*, "Enabling practical backscatter communication for on-body sensors," in *Proc. of the ACM SIGCOMM Conf.*, New York, NY, Aug. 2016, pp. 370–383.

[6] V. Iyer *et al.*, "Inter-technology backscatter: towards internet connectivity for implanted devices," in *Proc. of the ACM SIGCOMM Conf.*, Florianópolis, Brazil, Aug. 2016, pp. 356–369.

[7] A. Wang *et al.*, "FM backscatter: Enabling connected cities and smart fabrics," in *Proc. of the 14th USENIX Conf. on Netw. Syst. Des. and Implementation*, Mar. 2017, pp. 243–258.

[8] Y. Peng *et al.*, "PLoRa: A passive long-range data network from ambient LoRa transmissions," in *Proc. of the ACM SIGCOMM Conf.*, Aug. 2018, pp. 147–160.

[9] R. Duan *et al.*, "On the achievable rate of bi-static modulated re-scatter systems," *IEEE Trans. Veh. Technol.*, vol. 66, no. 10, pp. 9609–9613, Oct. 2017.

[10] G. Wang *et al.*, "Uplink detection and BER analysis for ambient backscatter communication systems," in *Proc. IEEE Global Commun. Conf. (GLOBECOM)*, San Diego, CA, Dec. 2015.

[11] Z. Mat *et al.*, "Signal detection for ambient backscatter system with multiple receiving antennas," in *Proc. IEEE 14th Canadian Workshop on Inform. Theory (CWIT)*, St. John's, NL, Canada, Jul. 2015, pp. 50–53.

[12] J. Qian *et al.*, "Noncoherent detections for ambient backscatter system," *IEEE Trans. Wireless Commun.*, vol. 16, no. 3, pp. 1412–1422, Mar. 2017.

[13] ——, "Semi-coherent detection and performance analysis for ambient backscatter system," *IEEE Trans. Commun.*, vol. 65, no. 12, pp. 5266–5279, Dec. 2017.

[14] G. Yang and Y. C. Liang, "Backscatter communications over ambient OFDM signals: transceiver design and performance analysis," in *Proc. IEEE Global Commun. Conf. (GLOBECOM)*, Washington, DC, Dec. 2016, pp. 1–6.

[15] M. A. ElMossallamy *et al.*, "Backscatter communications over ambient ofdm signals using null subcarriers," in *Proc. IEEE Global Commun. Conf. (GLOBECOM)*, Abu Dhabi, UAE, Dec. 2018, pp. 1–6.

[16] D. Darsena *et al.*, "Modeling and performance analysis of wireless networks with ambient backscatter devices," *IEEE Trans. Commun.*, vol. 65, no. 4, pp. 1797–1814, Apr. 2017.

[17] M. A. ElMossallamy *et al.*, "Noncoherent backscatter communications over ambient ofdm signals," in *IEEE Trans. on Commun., to be published*. [Online]. Available: http://dx.doi.org/10.1109/TCOMM.2019.2899301

[18] Y. P. E. Wang *et al.*, "A primer on 3gpp narrowband internet of things," *IEEE Communications Magazine*, vol. 55, no. 3, pp. 117–123, Mar. 2017.

[19] A. Ghosh *et al.*, *Fundamentals of LTE*, 1st ed. Upper Saddle River, NJ: Prentice Hall Press, 2010.

[20] J. F. Ensworth and M. S. Reynolds, "Every smart phone is a backscatter reader: Modulated backscatter compatibility with bluetooth 4.0 low energy (BLE) devices," in *IEEE Int. Conf. on RFID (RFID)*, San Diego, CA, Apr. 2015, pp. 78–85.

[21] J. Proakis and M. Salehi, *Digital Communications, 5th Edition*, 5th ed. McGraw-Hill Education, 2007.

[22] I. S. Ansari *et al.*, "On the sum of gamma random variates with application to the performance of maximal ratio combining over nakagami fading channels," in *IEEE 13th Int. Workshop on Signal Process. Advances in Wireless Commun. (SPAWC)*, Cesme, Turkey, Jun. 2012, pp. 394–398.

[23] Wolfram Research Inc., *The Wolfram Functions Site*. [Online]. Available: http://functions.wolfram.com